

A Systematic Description of the Generation of Covariance Matrices

N. M. Larson,* L.C. Leal, H. Derrien, G. Arbanas, R. O. Sayer, and D. Wiarda
Oak Ridge National Laboratory, P.O. Box 2008, Oak Ridge, Tennessee 37831 USA

Abstract

In this paper, we describe techniques used to determine realistic and appropriate uncertainties and correlations (or, equivalently, covariances) for multigroup cross sections in the resolved-resonance region, starting from fundamental principles. The entire process is described, with emphasis on the propagation of uncertainties through each step of the process. The key steps are data reduction (conversion from measured counts-per-time-channel to experimental cross section as a function of energy), data evaluation (determining appropriate parameter values to fit theory to experiment), generation of point-wise cross sections (reconstruction of theoretical cross sections as a function of energy), collapsing into multigroup cross sections (averaging the point-wise cross sections to give multigroup cross sections), and calculating integral quantities from those multigroup cross sections.

KEYWORDS: *Uncertainty, covariance, correlation, data analysis, nuclear data, R-matrix*

1. Introduction

Although the importance of covariances has been recognized by the nuclear community, there appears to be limited understanding of the nature of covariances and the manner in which they contribute to the solution of physical problems. This paper is an attempt to provide a systematic description of the various sources of uncertainty, their contributions to covariance matrices (CMs), and the effect they may have on the calculated values and uncertainties of integral quantities such as k_{eff} .

Our intent is to elucidate some important, but often overlooked, properties of CMs. First, one must recognize that the set of quantities (data, parameters, etc.) associated with the CM must be specified, in order for the term “covariance matrix” to be meaningful. For example, the CM associated with the energy-differential experimental cross sections provides a measure of the uncertainty on each individual data point (cross section at a particular energy) and of the relationship (correlation) between those data points. In this paper, we discuss techniques used to determine realistic and appropriate CMs associated with quantities of interest at the many different stages of nuclear data processing, starting from measurement of the raw data leading to energy-differential neutron cross sections, through the final calculation of integral quantities. Uncertainties are propagated through each step of the process.

* Corresponding author, Tel. 865-574-4659, Fax 865-574-8481, E-mail LarsonNM@ornl.gov

In the resonance region, ENDF/B data are generally stored as R-matrix parameters. The parameter values and the associated covariance matrix (uncertainties plus correlations) are frequently obtained using the SAMMY code [1], by fitting all available experimental data via a generalized least-squares technique (Bayes' method) in conjunction with (a) the Reich-Moore approximation to R-matrix theory and (b) corrections for experimental conditions. Hence, the evaluation of experimental data (neutron transmissions or total cross sections, capture, fission, or reaction cross sections) incorporates uncertainties in the experimental data. These uncertainties arise from a variety of sources, including both statistical uncertainties associated with the measurement itself and systematic uncertainties inherent in measurements of normalization, background, neutron time of flight, flight-path length, sample thickness, etc. All these uncertainties are included in the evaluation process, in order to properly determine the resonance-parameter covariance matrix (RPCM).

Pointwise cross sections are constructed from the R-matrix cross section formulae (Reich-Moore approximation) using the evaluated resonance parameters; the cross section covariance matrix (CSCM) for the pointwise cross sections is generated by propagating the RPCM through the R-matrix formulae. Group cross sections are obtained by weighting the pointwise cross sections with a neutron flux spectrum and integrating; the associated covariance matrix is found by propagating the CSCM through that process. Finally, calculations of k_{eff} and other integral quantities make use of either the pointwise cross sections or the group cross sections; uncertainties in those integral quantities are determined by propagating the covariance matrices associated with the cross sections.

In this paper, we discuss both how the resonance parameter covariance matrix (RPCM) is determined prior to inclusion in ENDF, and how it may be used afterward. Equations are presented when required for clarity; emphasis is on description rather than mathematical rigor.

2. Description of the Processes

In this section, the reader will note the frequent appearance of brackets containing asterisks and numbers {*1}. These are used to denote approximations whose inexactness will have consequences that will be discussed in Sect. 4.

2.1 Data Reduction Process

Measurement of cross section data is normally accomplished by time-of-flight techniques, in which a neutron beam bombards a sample containing the nuclide of interest, and particles exiting the sample are counted as a function of the time required for the neutron to traverse the distance from the neutron-producing target to the detector. The raw data are therefore the counts vs. time of flight. The time of flight is divided into bins or channels of equal or varying lengths, so that the actual data are "counts per time channel."

Conversion from raw data to reduced data is necessary to extract meaningful information from the measurement. Counts are converted to experimental cross sections (or to experimental transmissions) by correcting for detector dead time, subtracting backgrounds, normalizing with respect to the duration of the experiment, and so on. Time of flight t_i is converted to incident neutron energy E_i by the usual relationship

$$E_i = mL^2 / 2t_i^2 \quad , \quad (1)$$

in which m represents the mass of the incident neutron and L the flight-path length. {*1}

Raw data obey Poisson statistics. Essentially, this means that, if there are N counts for a given channel, the uncertainty on N is the square root of N . When the number of counts is large (as is often the case), it is adequate to treat a Poisson distribution as a normal distribution {2}. Each raw data point is independent of the other raw data points; that is, the number of counts in one channel is not correlated with the number of counts in any other channel {3}.

Reduced data, however, are no longer independent. This is most easily seen by considering relatively simple corrections such as normalization and background subtraction [1,2]. Normalization a and background b are measured by separate experiments; they each have uncertainties associated with them, which are expressed as Δa and Δb , respectively. (For simplicity, we shall assume that both a and b are constants rather than functions of time; the generalization is straightforward.) Uncertainties in a and b are propagated to the reduced data (the experimental cross sections), which we shall call d . Hence the reduced data d_1 at energy E_1 is related to the reduced data d_2 at E_2 ; this relationship is described via the experimental data covariance matrix, which we call V .

If r_i is the raw datum at time t_i and d_i is the corresponding experimental cross section at energy E_i , the energy is related to the time by Eq. (1) and the cross section to the raw datum by

$$d_i = (r_i - b) / a \quad . \quad (2)$$

Because uncertainties are known for all quantities on the right-hand-side of Eq. (2), it is possible to determine the covariance matrix for the experimental cross section. We begin by taking small increments of Eq. (2),

$$\delta d_i = (\delta r_i - \delta b) / a - (r_i - b) \delta a / a^2 = [\delta r_i - \delta b - d_i \delta a] / a \quad . \quad (3)$$

Next, multiply δd_i by δd_j and take expectation values,

$$\langle \delta d_i \delta d_j \rangle = \langle [\delta r_i - \delta b - d_i \delta a] [\delta r_j - \delta b - d_j \delta a] \rangle / a^2 = \{ \langle \delta r_i \delta r_j \rangle + \langle \delta^2 b \rangle + d_i d_j \langle \delta^2 a \rangle \} / a^2 \quad , \quad (4)$$

in which we have omitted the cross terms, because of the assumption that all the different quantities were measured in separate experiments and are therefore uncorrelated {4}. Finally, the experimental data covariance matrix can be written as

$$V_{ij} = \langle \delta d_i \delta d_j \rangle = \{ \Delta^2 r_i \delta_{ij} + \Delta^2 b + d_i d_j \Delta^2 a \} / a^2 \quad . \quad (5)$$

For a detailed description of the data-reduction process with application to natural Ni, see references [3] and [4].

2.2 Data Analysis or Evaluation

Neither raw nor reduced data are the appropriate quantities for use in nuclear reactor or transport calculations. Rather, what are needed are the *evaluated* cross sections, which reflect the “best” measured cross section value and also the best theoretical knowledge both of the shape of the “true” cross sections (e.g., R-matrix theory) and of the real-world modifications to the true cross sections (e.g., resolution or Doppler broadening, finite-size effects in the resolved resonance region; different examples apply for higher-energy regions.) Sophisticated computer codes such as SAMMY [1] are used to determine a best-fit set of resonance parameters and the associated CM. This CM reflects the statistical experimental uncertainties from the data reduction process and also includes systematic uncertainties related to the corrections for real-world effects {5}.

Let P_0 represent the initial estimates for the R-matrix parameters, and M_0 the corresponding parameter CM. Let T represent the theoretical cross section, including corrections for experimental conditions, and G the partial derivatives of T with respect to the parameters (i.e., G is the sensitivity matrix). Then the generalized least-squares equations used to calculate the evaluated set of R-matrix parameters (which we will call P) and the associated parameter CM (which we will call M) have the form {*6 }

$$P = P_0 + M G V^{-1} (d - T) \quad \text{and} \quad M = (G^t V^{-1} G + M_0^{-1})^{-1} \quad , \quad (6)$$

where V is the covariance matrix for the reduced data, from Eq. (5). [When $M_0^{-1} = 0$, the equations in (6) become the usual least-squares equations.]

All available data of all types (e.g., capture, elastic, total, fission or other reaction, both angle-integrated and angle-differential) are included in this fitting procedure, and the full off-diagonal data CM is used for each data set. When available, integral constraints such as resonance integrals, thermal cross sections, or g-factors are also included here.

The parameter set P is written into ENDF File 2 and the associated resonance parameter covariance matrix M is written into ENDF File 32. (In higher-energy regions, ENDF formats do not exist for comparable parameterization of the cross sections. Instead, pointwise cross sections are written into File 3 and the associated covariance matrix into File 33.)

2.3 Conversion to Pointwise Cross Sections

Processor codes such as AMPX [5] or NJOY [6] calculate pointwise cross sections (i.e., cross sections as a function of energy) directly from the R-matrix parameters, on an energy grid that is sufficiently dense to define all structure in the cross section. The associated CM can also be generated, using the sensitivity matrix (the partial derivatives of the cross sections with respect to the resonance parameters) to propagate uncertainty information stored in the resonance-parameter covariance matrix (RPCM). The resulting pointwise cross section CM will, in general, bear little resemblance to the CM for the reduced data discussed in Sect. 2.3, but it nevertheless incorporates the same information (plus much more, from the analysis process).

Let σ represent the pointwise cross section and U the associated covariance matrix. To propagate the covariance matrix M for P into U , we first take small increments in σ and use the chain rule for partial derivatives,

$$\delta \sigma(E) = \sum_i \frac{\partial \sigma(E)}{\partial P_i} \delta P_i \equiv \sum_i G_i(E) \delta P_i \quad , \quad (7)$$

where G is defined as the sensitivity matrix, which can be calculated analytically from the R-matrix formula for the cross section. Multiplying by $\delta \sigma(E')$ and taking expectation values gives

$$U(E, E') = \langle \delta \sigma(E) \delta \sigma(E') \rangle = \sum_{ij} G_i(E) \langle \delta P_i \delta P_j \rangle G_j(E') \quad , \quad (8)$$

in which $\langle \delta P_i \delta P_j \rangle$ is the RPCM element M_{ij} . Equation (8) can therefore be rewritten as

$$U(E, E') = \sum_{ij} G_i(E) M_{ij} G_j(E') \quad . \quad (9)$$

2.4 Averaging to Give Multigroup Cross Sections and Covariance Matrix

The pointwise cross sections and associated CM are averaged using an energy-dependent flux to give multigroup cross sections and the associated CM. Two codes used for this purpose are PUFF [7] and ERRORJ [8]. SAMMY [1] can also produce certain types of multigroup results in the resolved-resonance region and has been used for comparison studies with the other two codes.

A general equation for calculating the group-average cross section $\bar{\sigma}_g$ is

$$\bar{\sigma}_g = \int_{E_g}^{E_{g+1}} \sigma(E) \Phi(E) dE \quad \text{with} \quad \int_{E_g}^{E_{g+1}} \Phi(E) dE = 1 \quad , \quad (10)$$

in which $\Phi(E)$ is the normalized energy-dependent flux. Numerical integration algorithms are used to calculate $\bar{\sigma}$ {7}. If \bar{U} represents the covariance matrix associated with $\bar{\sigma}$, then

$$\begin{aligned} \bar{U}_{gg'} &= \langle \delta \bar{\sigma}_g \delta \bar{\sigma}_{g'} \rangle = \left\langle \int_{E_g}^{E_{g+1}} \Phi(E) \delta \sigma(E) dE \int_{E_{g'}}^{E_{g'+1}} \Phi(E') \delta \sigma(E') dE' \right\rangle \\ &= \int_{E_g}^{E_{g+1}} \Phi(E) dE \int_{E_{g'}}^{E_{g'+1}} \Phi(E') dE' \langle \delta \sigma(E) \delta \sigma(E') \rangle \equiv \int_{E_g}^{E_{g+1}} \Phi(E) dE \int_{E_{g'}}^{E_{g'+1}} \Phi(E') dE' U(E, E') \quad . \end{aligned} \quad (11)$$

Computations required by this equation can be simplified by inserting Eq. (9), yielding

$$\begin{aligned} \bar{U}_{gg'} &= \int_{E_g}^{E_{g+1}} \Phi(E) dE \int_{E_{g'}}^{E_{g'+1}} \Phi(E') dE' \sum_{ij} G_i(E) M_{ij} G_j(E') \\ &= \sum_{ij} \int_{E_g}^{E_{g+1}} G_i(E) \Phi(E) dE M_{ij} \int_{E_{g'}}^{E_{g'+1}} G_j(E') \Phi(E') dE' \equiv \sum_{ij} \bar{G}_{gi} M_{ij} \bar{G}_{g'j} \quad , \end{aligned} \quad (12)$$

in which we have defined the group-averaged partial derivative as

$$\bar{G}_{gi} = \int_{E_g}^{E_{g+1}} G_i(E) \Phi(E) dE \quad . \quad (13)$$

2.5 Calculating Integral Quantities

The multigroup cross sections and associated CM found in the previous section are then used to calculate k_{eff} (or other integral quantities). The mathematics is well understood for propagating the multigroup cross section CM, yielding a reasonable estimate for the nuclear data component of the uncertainty on k_{eff} . When Monte Carlo methods are used to compute k_{eff} , the statistical uncertainty associated with the Monte Carlo computation is also well understood. {8}

3. A Simple Example

To better understand the processes described in the previous section, raw data have been simulated for two “measurements,” one being neutron capture and the other neutron

transmission. Each data set has 61 data points. (In a real evaluation, there will be several independent data sets and thousands, or even hundreds of thousands, of data points for each data set.) These data used only two resonances; the first has orbital angular momentum $l = 2$ and the second has $l = 1$. Values for the resonance parameters are given in Table 1. Resolution and Doppler broadening, normalization, background, and noise were added to the artificially generated raw data to simulate real-world conditions. The statistical uncertainty on each raw datum was then set to the square root of N , where N is the number of counts (the value of the raw datum).

3.1 Data Reduction Process

The raw data were then reduced to capture cross sections and transmissions, using “measured” values for the normalizations and backgrounds and for the corresponding uncertainties. To illustrate how use of the correct data covariance matrix can compensate for inaccuracies that may be found especially in older data sets, the assumed measured value of the background for the capture experiment was taken to be quite a bit larger than the value used to generate the data. Nevertheless, as will be seen below, correct resonance parameter values were obtained.

3.2 Data Analysis or Evaluation

The reduced data were analyzed simultaneously via least-squares, using initial values for the resonance parameters that were different from the values used to create the simulated data. Four techniques were used for the uncertainties: (1) SAMMY’s “propagated uncertainty parameter” (PUP) method, which correctly incorporates the measurement-related uncertainties into the data CMs; (2) using the explicit data CMs for both data sets, as described in Sect. 2.2; (3) keeping only the diagonal portion of the data CMs; (4) keeping only the systematic portion of the data CMs. Results for the six resonance parameters are shown in Table 1. Clearly the PUP method gives superior results, with each of the six parameter values agreeing within the errors with the “true” values (the values used to create the simulated data). The explicit method disagrees only for Γ_{2n} , while the two diagonal methods disagree in both Γ_{1n} and Γ_{2n} .

Table 1: Resonance parameter values for the data analysis step.

	“True” values	Initial values	PUP method	Explicit data CM	Diagonal DCM	Statistical only
E_1 (keV)	181.055	181.060	181.055 ± 0.001	181.060 ± 0.001	181.055 ± 0.002	181.055 ± 0.002
$\Gamma_{1\gamma}$ (eV)	0.642	0.640	0.636 ± 0.105	0.684 ± 0.107	0.632 ± 0.104	0.629 ± 0.061
Γ_{1n} (eV)	21.691	17.922	23.064 ± 1.511	20.239 ± 1.613	24.471 ± 1.387	24.574 ± 1.034
E_2 (keV)	181.300	181.300	181.300 ± 0.001	181.300 ± 0.001	181.300 ± 0.002	181.300 ± 0.001
$\Gamma_{2\gamma}$ (eV)	0.708	0.710	0.716 ± 0.085	0.752 ± 0.080	0.712 ± 0.071	0.706 ± 0.043
Γ_{2n} (eV)	20.249	21.988	21.646 ± 1.319	24.226 ± 1.208	23.825 ± 0.990	23.692 ± 0.750

3.3. Conversion to Pointwise Cross Sections

The resonance parameter values found in the previous section using the PUP method were used to construct capture and total pointwise cross sections and the associated CMs. Figure 1 shows the CM for the reduced capture data; Fig. 2 shows the very different CM for the pointwise capture data, using the same energy scale. Figure 3 shows the CM that would be found for the pointwise capture data if the off-diagonal elements of the RPCM were not used; note the marked absence of the secondary peaks seen in Fig. 2.

Figure 1: Covariance matrix for the simulated experimental capture cross section.

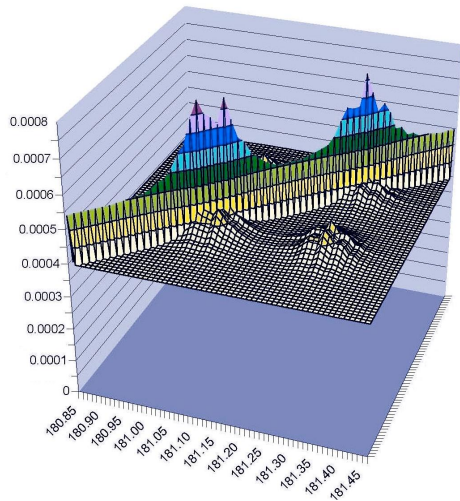


Figure 2: Covariance matrix for the pointwise capture cross section.

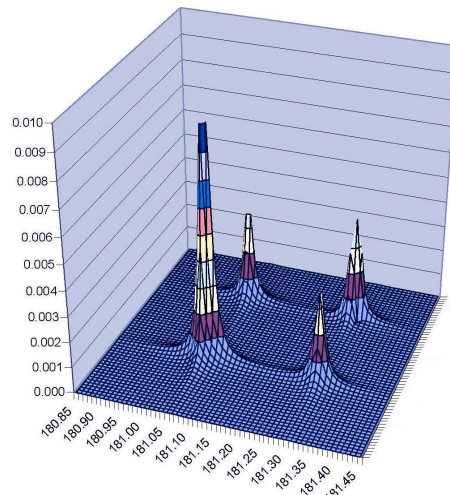
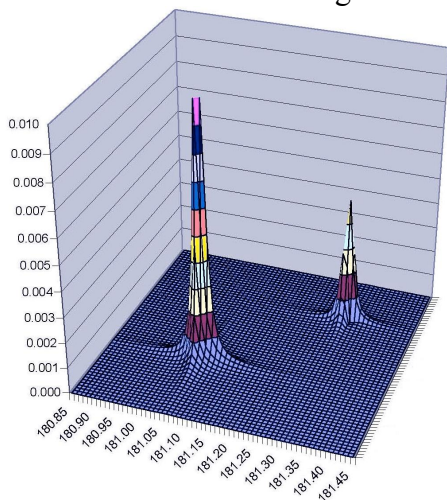


Figure 3: Covariance matrix for pointwise capture cross section, when off-diagonal components of the resonance parameter covariance matrix are neglected.



3.4 Averaging to Give Multigroup Cross Sections and Covariance Matrix

For this simple example, we somewhat arbitrarily choose two energy groups for averaging; the flux $\Phi(E)$ is taken to be independent of energy. Table 2 shows the multigroup averages, uncertainties, and correlation coefficients between the two groups when the full RPCM is used (as shown for the pointwise capture cross section in Fig. 2), and when off-diagonal components of the RPCM are neglected (as shown for the pointwise capture cross section in Fig. 3). While the values and uncertainties for the multigroup averaged cross sections do not differ too much for the two cases, the correlations are extremely different.

Table 2: Multigroup averages

Energy range (keV)	Using full RPCM		Using diagonal portion of RPCM	
	$\bar{\sigma}^{\text{capture}}$ (barns)	$\bar{\sigma}^{\text{total}}$ (barns)	$\bar{\sigma}^{\text{capture}}$ (barns)	$\bar{\sigma}^{\text{total}}$ (barns)
180.85 – 181.20	0.0803 ± 0.0104	7.514 ± 0.164	0.0803 ± 0.0103	7.514 ± 0.161
181.20 – 181.45	0.0628 ± 0.0088	6.535 ± 0.131	0.0628 ± 0.0086	6.535 ± 0.126
correlation	0.72	0.65	0.05	0.09

3.5 Calculating Integral Quantities

With this simple example, it is of course not possible to calculate k_{eff} or other integral values corresponding to physically meaningful quantities. It is possible, however, to study the effect of improper treatments of covariance matrices by calculating integrals of the type

$$F = \int \sigma(E) f(E) dE / \int f(E) dE , \tag{14}$$

where $f(E)$ assumes a variety of functional forms as shown in Table 3, and $\sigma(E)$ represents the pointwise cross sections of Sect. 3.3. The uncertainty on F is found by analogy with Eqs. (10) through (13). Table 4 shows results of these calculations; note that uncertainties are unrealistically high because of the artificial nature of this example.

Table 3: Functional forms used in calculations of pseudo integral quantities

i	$f_i(E)$
1	1
2	$E - E_{\text{min}}$
3	$(E - E_{\text{min}})^3$
4	$\sqrt{E} - \sqrt{E_{\text{min}}}$
5	$(E - E_{\text{min}} - 0.01\text{keV})^{-1}$
6	$\exp\left\{-\left[\frac{(E - E_{\text{mid}})}{(E_{\text{max}} - E_{\text{min}})}\right]^2\right\}$

In all cases, omitting the off-diagonal portion of a covariance matrix [either the RPCM or the cross section covariance matrix (CSCM)] results in uncertainties on the pseudo integral quantity that are significantly smaller than the more rigorous value. In our experience, a rigorously calculated uncertainty will be different from a more crude calculation, but sometimes larger and sometimes smaller. The only generalization that can be drawn is that the uncertainty on an integral quantity will not be calculated accurately when components of the covariance matrix are neglected.

Table 4: Calculations of pseudo-integral quantities and associated uncertainties, using various treatments of the cross section covariance matrix. Units are millibarns.

	$f_1(E)$	$f_2(E)$	$f_3(E)$	$f_4(E)$	$f_5(E)$	$f_6(E)$
Value of F	73.04	71.28	53.18	71.29	42.36	83.17
ΔF with full RPCM	9.07	8.98	7.17	8.98	5.35	10.32
ΔF with diagonal portion of RPCM	7.13	6.94	6.38	6.94	4.56	8.23
ΔF with diagonal portion of CSCM	1.00	1.02	0.97	1.02	0.59	1.16

4. Neglected Components of Covariance Matrices

In the previous section, we saw that neglect of any component of a covariance matrix can lead to erroneous results when that covariance matrix is used in further calculations. It is therefore of interest to consider what components might still be missing, even when great care is taken to properly include all known contributors. In Section 2, eight possibilities were indicated with a curly bracket containing an asterisk and a number. Here we provide information about the missing components alluded to there.

{*1} Often, the neutron is sufficiently energetic that relativistic effects are noticeable. While the conversion from time-of-flight to energy is usually done with relativistic equations, R-matrix analyses usually do not take relativistic kinematics into account.

{*2} The least-squares equations used for data fitting implicitly assume that all relevant quantities (experimental data, R-matrix parameters, etc.) obey Gaussian distributions (sometimes called “normal” distributions). The raw data, however, actually obey Poisson distributions. At high count rate, the Poisson distribution is indeed very similar to the normal distribution, so the approximation is good for the measurement of the resonance peaks in capture experiments and of the region between peaks in transmission experiments. At low count rate, however, the distribution is highly skewed from normal, which may cause difficulty in fitting the low cross sections between resonances for capture experiments, and very near the peaks of large resonances in transmission experiments.

{*3} While each raw data measurement is essentially independent of all other such measurements, there are certain interrelationships whose effect is usually neglected. For example, there is a dead time for the detector after measuring each event. The dead-time correction is universally taken to be absolute, with zero uncertainty; however, fluctuations in beam strength from one pulse to the next will produce small correlations between neighboring data points. To our knowledge, systematic uncertainties such as these are not yet incorporated into analysis codes.

{*4} Additional systematic uncertainties may occur due to the particular facility at which the experiments are performed. Uncertainties pertaining to data-processing hardware or software have not been studied.

{*5} The uncertainty in the model itself (R-matrix theory plus corrections for experimental conditions) has not yet been adequately explored. Mis-assigned quantum numbers, missed small resonances, and omitted noncompound processes (e.g., direct capture) contribute to the uncertainty in the calculation, as do approximations in resolution broadening, Doppler broadening, or other corrections for experimental effects. One immeasurable uncertainty involves the computer program itself; methods have not been developed for assigning uncertainty to undiscovered programming bugs.

{*6} The least-squares equations shown in (6) inherently assume that the theory is linear with respect to the parameters, an assumption which is clearly invalid for R-matrix parameters. In practice, the least-squares equations are generalized to include iteration for nonlinearity. Nevertheless, the use of an essentially linear treatment for an essentially nonlinear system may have implications for the uncertainty calculations.

{*7} The integrations described in Eqs. (10) through (13) are evaluated using numerical integration schemes. Any such scheme has an uncertainty associated with it.

{*8} Two components of uncertainty are generally omitted or ignored in integral calculations: the uncertainty associated with the model used to calculate the integral quantity and the

uncertainty associated with the use of multigroup cross sections rather than pointwise cross sections. Undiscovered programming bugs play a factor here just as they do in the analysis programs.

5. Summary

A description has been given of the various processes involved in measuring, reducing, analyzing, averaging, and using cross section data in the resolved-resonance region, with particular attention to the uncertainties at each step of the process. The ideas expressed in that description were illustrated with a simple example. Neglected components of uncertainty were discussed.

While this paper serves to illustrate the current status of the treatment of covariances, further work is clearly indicated. More realistic examples should be studied, and extensions into the higher-energy regions included. Methodologies should be developed to describe the neglected components.

Acknowledgments

This work was performed with support from the U.S. DOE Nuclear Criticality Safety Program (NNSA/NA-11).

References

- 1) N. M. Larson, "Updated users' guide for SAMMY: multilevel R-matrix fits to neutron data using Bayes= equations," ORNL/TM-9179/R7, Oak Ridge National Laboratory (2006).
- 2) N. M. Larson, "Treatment of data uncertainties," ND2004, International Conference on Nuclear Data for Science and Technology, Sept. 26-Oct. 1, 2004, p. 374.
- 3) D. C. Larson, N. M. Larson, J. A. Harvey, N. W. Hill, and C. H. Johnson, "Application of new techniques to ORELA neutron transmission measurements and their uncertainty analysis: the case of natural nickel from 2 keV to 20 MeV," ORNL/TM-8203, ENDF-333 (1983).
- 4) N. M. Larson, "User's guide to ALEX: uncertainty propagation from raw data to final results for ORELA transmissions measurements," ORNL/TM-8676, ENDF-332 (February 1984).
- 5) M. E. Dunn and N. M. Greene, "AMPX-2000: A cross-section processing system for generating nuclear data for criticality safety applications," Trans. Am. Nucl. Soc. (2002).
- 6) R. E. MacFarlane et al., "The NJOY nuclear data processing system," LA-9303-M, Vol. II (ENDF-324) (1982).
- 7) D. Wiarda, M. E. Dunn, N. M. Greene, N. M. Larson, and L. C. Leal, "New capabilities for processing covariance data in resonance region," this conference, 2006. See also J. D. Smith III, "Processing ENDF/B-V uncertainty into multigroup covariance matrices," ORNL/TM-7221, Union Carbide Corp., Oak Ridge National Laboratory (June 1980) and M.E. Dunn, "PUFF-III: a code for processing ENDF uncertainty data into multigroup covariance matrices," ORNL/TM-1999/235 or NUREG/CR-6650 (1999).
- 8) G. Chiba, "ERRORJ-covariance processing code system for JENDL, version 2," JNC TN9520 2003-008.